Surface effects in color superconducting strangelets and strange stars

Micaela Oertel, Michael Urban

Surface effects in color superconducting strangelets and strange stars

Micaela Oertel
LUTH, Observatoire de Paris, CNRS, Université Paris Diderot, 5 place Jules Janssen, 92195 Meudon, France

Michael Urban
IPN Orsay, CNRS-IN2P3 and Université Paris-Sud, 91406 Orsay cedex, France

Surface effects in strange-quark matter play an important role for certain observables which have been proposed in order to identify strange stars, and color superconductivity can strongly modify these effects. We study the surface of color superconducting strange-quark matter by solving the Hartree-Fock-Bogoliubov equations for finite systems ("strangelets") within the MIT bag model, supplemented with a pairing interaction. Due to the bag-model boundary condition, the strange-quark density is suppressed at the surface. This leads to a positive surface charge, concentrated in a layer of ~ 1 fm below the surface, even in the color-flavor locked (CFL) phase. However, since in the CFL phase all quarks are paired, this positive charge is compensated by a negative charge, which turns out to be situated in a layer of a few tens of fm below the surface, and the total charge of CFL strangelets is zero. We also study the surface and curvature contributions to the total energy. Due to the strong pairing, the energy as a function of the mass number is very well reproduced by a liquid-drop type formula with curvature term.

PACS numbers: 21.65.Qr,12.39.Ba,26.60.-c

I. INTRODUCTION

From rather general arguments it is expected that at low temperatures and high densities quark matter is in a color superconducting state [1]. More recently [2, 3] it has been suggested that the diquark pairing gaps for quark matter at densities of several times nuclear matter saturation density could be of the order of ~ 100 MeV. Since this could have important phenomenological consequences in particular for the interior of compact stars, this has triggered much work on color superconductivity in dense quark matter (for reviews, see, e.g., Ref. [4]). These investigations of the QCD phase diagram have revealed a very rich phase structure with many different possible pairing patterns, depending on external conditions such as, for instance, electrical neutrality or quark masses. The largest diquark pairing gaps arise from scalar condensates, leading either to the two-flavor (2SC) phase or to the color-flavor-locked (CFL) phase [5, 6]. The latter pairing pattern involves strange (s) quarks, in addition to the two light quark flavors, up (u) and down (d).

If color superconducting quark matter exists in nature, the most likely place to find it is the interior of compact stars because matter is compressed there to densities much higher than nuclear matter saturation density. However, it has been argued that strange-quark matter (SQM) might be absolutely stable [7]. Under this hypothesis, even pure strange stars should exist [8], i.e., stars entirely composed of SQM. Also small lumps of SQM, called "strangelets," might be stable. Because of their low charge to baryon number ratio Z/A, strangelets have been proposed to populate ultra high energy cosmic rays [9].

In SQM without pairing, the density of strange quarks is supposed to be smaller than that of light quarks because of their higher mass. Consequently, SQM and strangelets are positively charged and the charge neutrality of strange stars has to be achieved via the presence of electrons. At the surface an atmosphere of electrons forms [8] which can potentially be detected [10, 11] via the emission of electron-positron pairs from an extremely strong electric field at the surface.

Recently another possible picture of the surface of a strange star has been proposed [12]: there could be a "crust" composed of strangelets emerged in an electron gas. Similar to an ordinary neutron star, there could be an interface between the crust and the interior in form of the famous "pasta phases." Within this scenario the electric field at the surface would be strongly reduced. Obviously, surface effects for the strangelets play an important role for the description of this scenario. For instance, there is a critical surface tension deciding whether a homogeneous phase or the droplet phase is favored [13]. Another question for which surface effects should be considered is the formation of a strange star in a supernova explosion. Before the explosion the original star contains hadronic matter. During the formation of the star, nucleation of strangelets sets in, leading then to a conversion of the entire star to SQM. For the nucleation process the properties of small strangelets are important.

Pairing tends to reduce the differences in density of different quark species. For bulk quark matter in the CFL state, requiring color neutrality, all quarks are paired. The densities are thus equal and CFL quark matter is electrically neutral on its own, i.e. without any electrons [14]. This would suggest dramatic changes in the properties of strangelets and SQM inside compact stars. For instance, the electrosphere at the surface of a strange star could completely disappear. But, the presence of the surface can modify this picture since it can lead to a non-zero surface charge which remains even for large

objects. For example, the boundary condition of the MIT bag model suppresses the density of the massive strange quarks at the surface, resulting in a positive surface charge [15]. Within this scenario, the total charge of a strangelet, following roughly $Z \approx 0.3A^{2/3}$, is drastically reduced with respect to "normal" strangelets. For strange stars, this requires the presence of electrons [16]. However, pairing has not been treated self-consistently in previous work (see, e.g., Ref. [15]). Within this paper we will therefore reinvestigate finite-size strangelets with pairing by considering quark matter in a color superconducting spherical bag, solving the Hartree-Fock-Bogoliubov (HFB) equations. We will show, in particular, that there exist CFL type solutions where all quarks are paired and the total charge of the strangelet strictly vanishes.

The outline of the paper is as follows. In section II we will present our model for treating color superconducting quark matter in a finite volume. In section III we will show numerical results. In section III A we discuss the possibility of qualitatively different configurations. In section III B we concentrate on the charge-density distributions of the CFL like solutions. In section III C we discuss a liquid-drop like mass formua for the CFL-like solutions and calculate the surface tension. Finally, in section IV we will summarize our results.

II. MODEL

Since it is not possible to describe strangelets or SQM with a surface from first principles (QCD), we will use a quark model which allows to describe finite-size objects. For this purpose we will use here the simplest version of the MIT bag model [17]. The MIT boundary condition ensures that there is no particle flux across the surface of the (spherical) bag with radius R and can be written, for the quark field ψ, as

$$-i\mathbf{e}_r \cdot \boldsymbol{\gamma}\psi = \psi|_{r=R}\,. \tag{1}$$

This boundary condition, Eq. (1), leads to a suppression of the wave functions of massive particles at the surface. This means that the strange quark density will a priori be suppressed at the surface with respect to the light quark densities. We will work with quark masses $m_u = m_d = 0$ and $m_s = 120$ MeV.

In order to include pairing, we will supplement the bag model with a pairing interaction. Throughout this paper, we will consider only scalar color antitriplet diquark condensation, i.e., condensates of the form

$$s_{AA'}(x) = -\langle \bar{\psi_T}(x)\tau_A\lambda_{A'}\psi(x)\rangle\,, \tag{2}$$

where $\tau_A, \lambda_{A'}$ represent $SU(3)$ matrices in flavor and color space, respectively. We follow the convention that capital letters A, A' indicate that we are restricting $\{A, A'\}$ to be antisymmetric, i.e., in terms of the Gell-Mann matrices, $\{A, A'\} \in \{2, 5, 7\}$. By ψ_T we denote the time-reversed conjugate of ψ,

$$\psi_T(x) = \gamma_5 C\bar{\psi}^T(x)\,, \tag{3}$$

with C being the charge conjugation matrix. In uniform infinite matter and for an exact $SU(3)$ flavor symmetry, the CFL phase is characterized by nonzero values $s_{22} = s_{55} = s_{77}$, whereas the 2SC state has only $s_{22} \neq 0$. If we want to generalize this concept to a finite system, we have to consider the possibility that the condensates can be position dependent.

For simplicity we choose a pairing interaction of the form

$$\mathcal{L}_{qq} = H\sum_{A,A'}(\bar{\psi}i\gamma_5\tau_A\lambda_{A'}C\bar{\psi}^T)(\psi^T Ci\gamma_5\tau_A\lambda_{A'}\psi)\,. \tag{4}$$

This Lagrangian describes a four-point interaction with a dimensionful coupling constant H. It corresponds to a scalar quark-quark interaction in the color and flavor antitriplet channel, needed for giving rise to the diquark condensates s_{AA}.

The HFB equations are obtained from the Lagrangian by minimizing the energy in mean field approximation, i.e., linearizing the interaction under the assumption of nonzero values of the condensates s_{AA}. For our problem, the HFB equations read (for more details see Appendix B and Ref. [18] where the "Dirac-Hartree-Bogoliubov" approximation was developped for finite nuclei):

$$\begin{pmatrix} h & \Delta \\ \Delta & -h \end{pmatrix}\begin{pmatrix} U_\alpha(\mathbf{r}) \\ \gamma^0 V_\alpha(\mathbf{r}) \end{pmatrix} = \epsilon_\alpha \begin{pmatrix} U_\alpha(\mathbf{r}) \\ \gamma^0 V_\alpha(\mathbf{r}) \end{pmatrix}\,, \tag{5}$$

where h is the Dirac single-particle Hamiltonian, $h = -i\boldsymbol{\alpha}\cdot\boldsymbol{\nabla} + m_f\gamma^0 - \mu_{fc}$. Here, m_f denotes the mass for quarks of flavor $f \in \{u, d, s\}$ and μ_{fc} is the chemical potential for flavor f and color $c \in \{r, g, b\}$ (we will denote the three colors by red, green, and blue). The spinors U_α and V_α describe the particle- and hole-like components of the quark fields, respectively [see Eq. (B1)]. In writing Eq. (5) we implicitly assumed that the pairing field Δ can be chosen real, which is the case for the pairing pattern we consider. It is related to the condensates, Eq. (2), by the self-consistency condition

$$\begin{aligned}\Delta(\mathbf{r}) =& 2H\sum_{A=2,5,7} s_{AA}(\mathbf{r})\tau_A\lambda_A \\ =& 2H\sum_{A=2,5,7}\sum_{\beta(\epsilon_\beta<0)} \bar{V}_\beta(\mathbf{r})\tau_A\lambda_A U_\beta(\mathbf{r})\,.\end{aligned} \tag{6}$$

In practice, this expression is divergent and it is necessary to introduce a cutoff in order to obtain a finite result. Since in a finite system the levels are discrete, a sharp cutoff would generate discontinuities as a function of the system's size. We therefore introduce a smooth cutoff function $f(p/\Lambda)$ (see Appendix C for details). In the following discussion we will use $\Lambda = 600$ MeV. Another practical problem arises from antiparticle contributions. However, since the chemical potentials μ_{fc} are

large and positive and pairing involves mostly the states near the Fermi surface, we assume that the antiparticle contributions are not important and can be neglected. We checked this approximation (analogous to the "no-sea approximation" in nuclear physics [18]) in infinite matter and found that the effect of antiparticle states can be absorbed in a readjustment of the coupling constant by $\sim 20\,\%$.

The chemical potentials, μ_{fc}, are adjusted to achieve color neutrality, i.e., equal numbers of quarks for each color, and beta equlibrium. In an infinite homogeneous system the condition for beta equilibrium gives just a relation between the chemical potentials[1]

$$\mu_{dc} = \mu_{sc} = \mu_{uc} + \mu_e \qquad \text{for all } c\,. \tag{7}$$

In a small system this is slightly different. First, even if there are any electrons (i.e., if the strangelet is charged), they are not localized inside the strangelet, but they form a large cloud like in ordinary atoms and hence their chemical potential μ_e is approximately equal to the electron mass and can be neglected. The second difference comes from the fact that particle numbers are discontinuous functions of the chemical potentials. The term beta equilibrium should now be replaced by beta stability, which means that the system does not gain energy by performing a beta decay, inverse beta decay, or electron capture, i.e., transforming an up- into a down- or strange quark or vice versa, accompanied by the corresponding leptons. To achieve beta stability, we therefore compare the energies of adjacent strangelets with the same total quark number, differing only in the number of up-, down-, and strange quarks, respectively. Of course, in the case of large particle numbers, the minimum energy configuration fulfils approximately the condition (7).

Within the bag model, the quark pressure in the bag is counterbalanced by the bag pressure B. Formally this can be written as

$$\frac{dE}{dV} = 0\,, \tag{8}$$

where $E = E_q + BV$ is the total energy, E_q is the energy of the quarks in the bag (including the interaction energy, which in our case comes from the pairing interaction) and $V = 4\pi R^3/3$ is the volume of the bag. Eq. (8) determines the radius of the strangelet for given bag pressure, interaction strength and particle number. We can get an idea of the value of the bag pressure if we look at the stability of bulk quark matter. Non-strange quark matter should be energetically less favored than normal hadronic matter, whereas SQM should be stable if for some baryon number $A > A_c$ strangelets become stable and consequently strange stars can exist. This means that we want the energy per baryon of SQM to be less than 931 MeV, the energy per baryon of the most stable nucleus, ^{57}Fe. On the other hand, the energy per baryon of non-strange quark matter should be larger than the nucleon mass. Without interaction the window for the values of the bag constant is then 148 MeV $< B^{1/4} <$ 157 MeV. These values change as a function of the interaction strength H. To better compare the results, we will readjust for each coupling strength the bag constant in order to get $E/A = 900$ MeV. The corresponding values are listed in Table I, together with other properties of infinite matter. Non-strange quark matter is unstable with these parameter values. Note that for the weakest non-vanishing coupling constant given in Table I, SQM is in the 2SC phase and not in the CFL phase. For the larger coupling constants, the CFL phase is preferred. Note that, due to the mass difference of light and strange quarks, the flavor $SU(3)$ symmetry is not exact and the gap Δ_2 is different from Δ_5 and Δ_7. However, since the CFL phase is electrically neutral, and we have $m_u = m_d = 0$, the isospin $SU(2)$ symmetry in the up- and down-quark sector is exact and therefore $\Delta_5 = \Delta_7$.

TABLE I: Values of the bag constants for different values of the coupling constant H, resulting in color and electrically neutral SQM with electrons in beta equilibrium with an energy per baryon of $E/A = 900$ MeV. The corresponding baryon densities ρ_B, electron densities ρ_e, and pairing gaps in infinite matter are also displayed.

$H\Lambda^2$	$B^{1/4}$ (MeV)	ρ_B (fm^{-3})	ρ_e (fm^{-3})	Δ_2 (MeV)	$\Delta_5 = \Delta_7$ (MeV)
0	152.03	0.329	7.3×10^{-6}	0	0
1.5	152.44	0.339	9.7×10^{-5}	27.7	0
1.75	153.97	0.367	0	35.1	34.5
2	156.26	0.395	0	50.6	49.7
2.25	159.46	0.427	0	67.2	66.0
2.5	163.46	0.463	0	84.6	83.1

In addition to the strong interaction, the quarks will exhibit electromagnetic interactions which, due to their long range, become in particular important for large objects. We will include only the direct (Hartree) term of the Coulomb interaction, which is given by

$$A^0(r) = e \int d^3r' \frac{\rho_{ch}(r')}{|\mathbf{r} - \mathbf{r}'|}\,, \tag{9}$$

where $\rho_{ch} = (2\rho_u - \rho_d - \rho_s)/3$ is the charge density (divided by e), ρ_f being the number density of quarks of flavor f.

It would be in the spirit of the bag model to include also the gluon exchange in a perturbative way, i.e., as a first approximation, in the same way as the photon. However, this goes beyond the scope of the present paper and will be postponed to a forthcoming publication.

[1] Here we assume that neutrinos are not trapped, i.e., they can freely leave the system

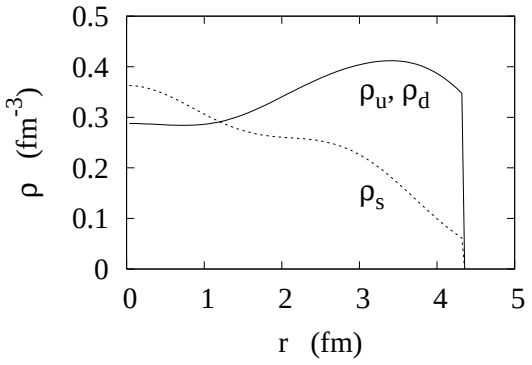

FIG. 1: Quark number density profiles of the strangelet $A = 108$, $Z = 24$ in the case of vanishing pairing interaction (free quarks in a bag) and $B^{1/4} = 152.03$ MeV.

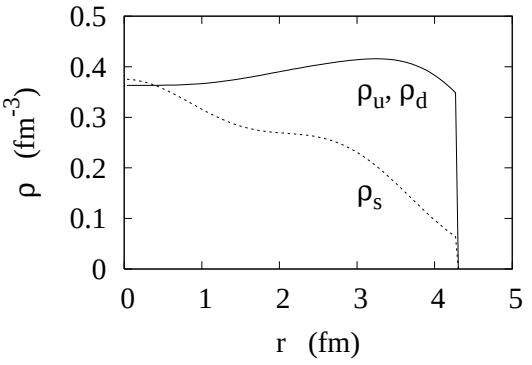

FIG. 2: Quark number density profiles of the strangelet $A = 108$, $Z = 24$ in the case of $H\Lambda^2 = 1.5$ and $B^{1/4} = 152.44$ MeV.

III. RESULTS

A. Different types of solutions

We will first discuss the qualitatively different configurations we find. In small strangelets, the effect of Coulomb interaction is in general very small, such that the general features discussed within this section are not modified if we include the Coulomb term. We will therefore present here for simplicity results switching off the Coulomb interaction. Coulomb interaction will become important when we discuss the charge density distributions of large objects in section III B.

Let us start by discussing a small strangelet ($A = 108$, $Z = 24$) without any pairing interaction ($H\Lambda^2 = 0$). The quark numbers and other relevant information are listed in Table II. As expected, due to the finite size of the bag, the energy per baryon ($E/A = 931.5$ MeV) is much higher than that of color neutral infinite matter with $\mu_{uc} = \mu_{dc} = \mu_{sc}$[2] ($E/A = 899.5$ MeV). This effect will be discussed in more detail in section III C. The density profiles of light and strange quarks are shown in Fig. 1. As expected, due to the boundary condition, the strange-quark density is strongly suppressed at the surface, contrary to the densities of the light quarks. For comparison we mention that for the same value of the bag constant, the densities in color neutral infinite matter with $\mu_{uc} = \mu_{dc} = \mu_{sc}$ are: $\rho_u = \rho_d = 0.355$ fm^{-3}, $\rho_s = 0.274$ fm^{-3}. We see that not only the strange-quark density, but also the densities of the light quarks are quite different from these values and depend strongly on r because of the existence of discrete levels in the bag.

Now we switch on the pairing interaction. In the case of $H\Lambda^2 = 1.5$, SQM is in the 2SC phase, i.e., only up and down quarks of two colors (red and green in our notation) are paired. This is also true in a finite strangelet. Therefore it is clear that the strange-quark density profile remains the same as without pairing. The oscillations of the densities of the light quarks, however, are much weaker now than in the case without pairing, since pairing washes out the occupation numbers. This can be seen in Fig. 2. In this 2SC-like solution, only one of the gaps, Δ_2, is non-zero. Since Δ_2 involves only the wave functions of up and down quarks, which are not suppressed at the surface, it extends up to the surface of the bag, as shown in Fig. 3. As a function of r, it is almost constant and quite close to the corresponding value in infinite matter with $\mu_{uc} = \mu_{dc} = \mu_{sc}$, which is $\Delta_2 = 29.2$ MeV.

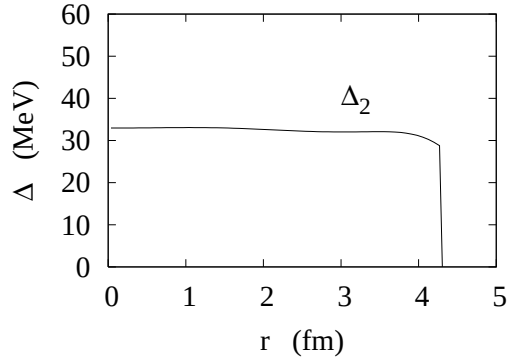

FIG. 3: Gap $\Delta_2(r)$ of the strangelet $A = 108$, $Z = 24$ in the case of $H\Lambda^2 = 1.5$ and $B^{1/4} = 152.44$ MeV.

If we increase the coupling constant to $H\Lambda^2 = 1.75$, we obtain three qualitatively different solutions which have comparable energies. The most stable one is still of the 2SC type, although in infinite matter the CFL phase is preferred. In this case, the strangelet still has $Z = 24$ and the density profiles are almost identical to those shown in Fig. 2. The main difference is that now the value of the gap is larger.

In the two other solutions, also strange quarks partic-

[2] As discussed below Eq. (7), it is more appropriate to compare a small strangelet with this kind of matter rather than with electrically neutral matter with electrons in beta equilibrium.

TABLE II: Parameters and properties of the strangelets discussed in section III A: B = bag constant, H = coupling constant of the pairing interaction, A = baryon number, Z = charge, N_{fc} = number of quarks of flavor f and color c, E/A = energy per baryon, R = radius of the bag, $\Delta_A(0)$ = value of the gap at $r = 0$.

$B^{1/4}$ (MeV)	$H\Lambda^2$ (MeV)	A	Z	$\begin{pmatrix} N_{ur} & N_{ug} & N_{ub} \\ N_{dr} & N_{dg} & N_{db} \\ N_{sr} & N_{sg} & N_{sb} \end{pmatrix}$	E/A (MeV)	R (fm)	$\Delta_2(0)$ (MeV)	$\Delta_5(0) = \Delta_7(0)$ (MeV)
152.03	0	108	24	$\begin{pmatrix} 44 & 44 & 44 \\ 44 & 44 & 44 \\ 20 & 20 & 20 \end{pmatrix}$	931.5	4.36	0	0
152.44	1.5	108	24	$\begin{pmatrix} 44 & 44 & 44 \\ 44 & 44 & 44 \\ 20 & 20 & 20 \end{pmatrix}$	929.7	4.31	33.0	0
153.97	1.75	108	24	$\begin{pmatrix} 44 & 44 & 44 \\ 44 & 44 & 44 \\ 20 & 20 & 20 \end{pmatrix}$	933.0	4.24	49.6	0
153.97	1.75	108	10	$\begin{pmatrix} 38 & 39 & 41 \\ 39 & 38 & 41 \\ 31 & 31 & 26 \end{pmatrix}$	934.6	4.21	41.6	24.9
153.97	1.75	108	0	$\begin{pmatrix} 38 & 35 & 35 \\ 35 & 38 & 35 \\ 35 & 35 & 38 \end{pmatrix}$	934.8	4.17	33.8	37.0

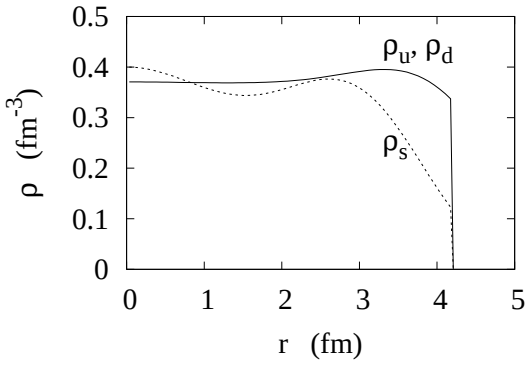

FIG. 4: Density profiles of the strangelet $A = 108$, $Z = 10$ in the case of $H\Lambda^2 = 1.75$ and $B^{1/4} = 153.97$ MeV.

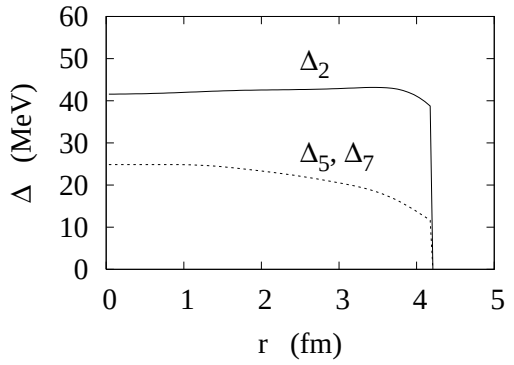

FIG. 5: Gaps Δ_A as functions of r for the strangelet $A = 108$, $Z = 10$ in the case of $H\Lambda^2 = 1.75$ and $B^{1/4} = 153.97$ MeV.

ipate in pairing ($\Delta_5 = \Delta_7 \neq 0$). These two solutions have charge $Z = 10$ and $Z = 0$, respectively. Let us first discuss the case $Z = 10$. In this case, there are a couple of u and d quarks which remain unpaired. The wave function of the unpaired level is mainly localized near the surface of the bag, as can be seen in Fig. 4, where the density profiles are shown. In the inner part, the densities of up, down, and strange quarks are almost equal, while near the surface, where the strange quark density is suppressed due to the boundary condition, there is an excess of up and down quarks. This excess is due to the unpaired quarks. The fact that one level of u and d quarks does not participate in pairing means that the occupation number of this level is equal to 1. At the same time, the corresponding level, i.e., with the same quantum numbers j and κ (see Appendix A) of the strange quarks has an occupation number equal to 0 (in the present case this level has $j = 9/2$, $\kappa = -5$). In a certain sense this situation is analogous to the "breached pairing" phase of infinite matter [19]. The charge Z is equal to the degeneracy $2j+1$ of the unpaired level. The gaps Δ_A as functions of r corresponding to this solution are displayed in Fig. 5.

In the third solution, all quarks are paired. As a consequence, the numbers of up, down, and strange quarks are equal, and the total charge is $Z = 0$. This is analogous to the CFL phase in the infinite system. Since the strange quark density is suppressed near the surface, but the number of strange quarks is equal to those of up and down quarks, it is clear that the strange-quark density must be larger than the up- and down-quark densities in some other part of the system. This is indeed the case, as can be seen in Fig. 6. We also see that the excess of the light-quark densities over the strange-quark density is reduced as compared with the case $Z = 10$ discussed above (cf. Fig. 4). We will discuss the charge-density distribution in detail in section III B. The gaps, shown in Fig. 7, are much closer to the gaps in infinite matter (cf. Table I) than in the case $Z = 10$.

For the larger values of the coupling constant we considered ($H\Lambda^2$ =2, 2.25,2.5), it is always the CFL-type solution ($Z = 0$) which has the lowest energy. We do not show any figures because in all these cases the results are analogous to those shown in Figs. 6 and 7, (just the values of the gaps change, they are close to those given in Table I for infinite matter).

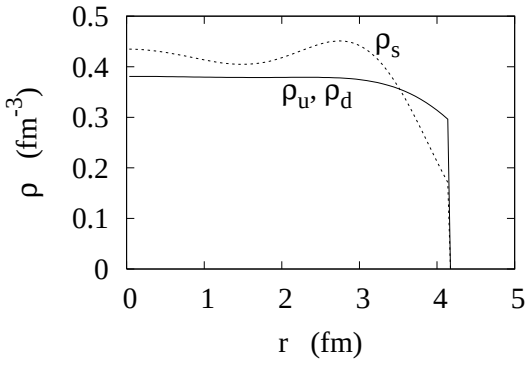

FIG. 6: Density profiles of the strangelet $A = 108$, $Z = 0$ in the case of $H\Lambda^2 = 1.75$ and $B^{1/4} = 153.97$ MeV.

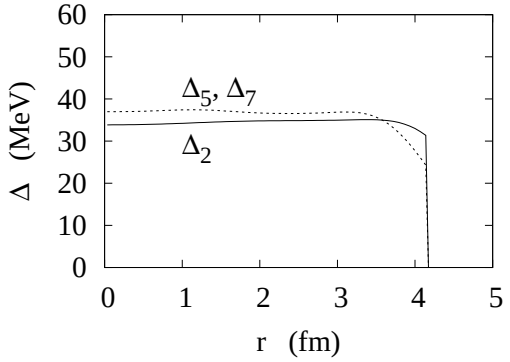

FIG. 7: Gaps Δ_A as functions of r for the strangelet $A = 108$, $Z = 0$ in the case of $H\Lambda^2 = 1.75$ and $B^{1/4} = 153.97$ MeV.

It should be mentioned that the fully paired solutions with $Z = 0$ are very robust as soon as the coupling constant is sufficiently large, i.e., we find this type of solution for arbitrary numbers of quarks[3]. This solution is in contrast to previous findings (see, e.g., Ref. [15]), where it was supposed that the CFL matter should be neutral in the bulk with just a thin positively charged surface layer with an excess of up and down quarks because of the boundary condition. In fact, this idea corresponds roughly to our solution with unpaired up and down quarks near the surface. This solution is, however, very fragile and exists only for certain values of parameters and mass numbers, since it requires the existence of a suitable level of light and strange quarks near the respective Fermi surfaces which can serve as unpaired level. Nevertheless, even in the case of strong coupling constants we encountered some exceptional cases where this kind of solution is energetically favored over the fully paired one.

[3] If the number of quarks is odd, it it impossible to pair all quarks and one or several state(s) should be "blocked" by the unpaired quark(s). At present, we have not included this effect in our calculation.

B. Charge density distribution

Within this section we will discuss the charge density distributions for the different configurations mentioned in the previous section. As expected, in all cases except the 2SC phase, pairing drastically reduces the total charge Z. Because of surface effects, the local charge density does, however, not vanish, even within the CFL-type solution which has $Z = 0$. Due to the suppression of the strange-quark wave function at the surface, a positively charged surface layer remains with an extension of ~ 1 fm, as has already been pointed out in Ref. [15].

Within the configuration with some unpaired light quarks at the surface, the total charge of the strangelet results from this positive surface charge, the interior of the strangelet has almost zero charge density. The total charge is here reduced compared with a strangelet without pairing, for example the $A = 108$ strangelet has $Z = 10$ within this paired configuration, whereas the corresponding unpaired strangelet has $Z = 24$. A systematic study of the total charge of strangelets in this configuration will not be discussed here since this configuration is rather fragile with respect to the details of the single-particle spectra and thus difficult to realize for many different particle numbers.

Let us therefore concentrate on the CFL-type solution, which exists for arbitrary particle numbers. Since all quarks are paired, we have equal numbers of up-, down-, and strange quarks such that the total charge of these strangelets is zero. The positive surface charge is mainly compensated by an excess of negative charge concentrated at around 1-3 fm below the surface. In addition, neglecting Coulomb interaction, we find an almost homogeneously negatively charged interior. Since the surface charge remains almost constant and the surface grows as R^2, whereas the volume grows as R^3, we expect the density of the negatively charged interior to decrease roughly as $1/R$. This is indeed the case, at least as long as the strangelet is not too large. Of course, one should ask, what will be the effect of electromagnetic interactions on this picture. Within our model, this concerns a pure Coulomb interaction. We have, however, to keep in mind, that in principle the mixing of the photon with one of the gluons should be considered. Below we will briefly comment on this issue.

In order to study the effect of the Coulomb interaction, we consider the CFL-type solution for strangelets of different mass numbers A from $A = 108$ to $A = 90000$, for one particular value of the coupling constant, $H\Lambda^2 = 2$. The direct (Hartree) term of the Coulomb interaction is now included. In order to reduce the considerable numerical effort, we use for the large strangelets (starting from $A = 15000$) the condition (7) with $\mu_e = 0$ (and as a consequence, the quark numbers for each flavor and color are not integers) instead of looking for the true energy minimum with respect to beta decay. In addition, we do not minimize the energy with respect to the radius, but we simply estimate the volume of the bag by dividing the

mass number A by the baryon density $\rho_{B\,bulk}$ of infinite matter. These two approximations are very accurate for such large strangelets. Already in the case of $A = 3000$, the quark numbers and the radius are very well reproduced within these approximations: the full minimization results in quark numbers $N_{ur} = N_{dg} = N_{sb} = 1052$, $N_{ug} = N_{dr} = N_{ub} = N_{sr} = N_{db} = N_{sg} = 974$, and a radius $R = 12.23$ fm, while the approximations lead to $N_{ur} = 1051.8$, $N_{dg} = 1051.7$, $N_{sb} = 1051.1$, $N_{ug} = N_{dr} = 973.8$, $N_{ub} = N_{sr} = 974.4$, $N_{db} = N_{sg} = 974.5$, and $R = 12.19$ fm.

Our results are shown in Figs. 8 and 9. We see that the Coulomb interaction pushes the negative charge towards the surface. Let us quantify this effect. If the system was semi-infinite with a plane surface at $z = 0$ (the system being situated at $z < 0$), we would expect the charge density to go to zero exponentially if one goes away from the surface. This can be seen as follows: We know that in the medium with Debye screening the (static) Poisson equation for the Coulomb potential is replaced by

$$\left(\boldsymbol{\nabla}^2 - \frac{1}{\lambda^2}\right) A^0 = 0\,, \tag{10}$$

where λ is the screening length. Taking the Laplacian of this equation, we see that the charge density obeys the analogous equation

$$\left(\boldsymbol{\nabla}^2 - \frac{1}{\lambda^2}\right) \rho_{ch} = 0\,. \tag{11}$$

The solution of this equation which goes to zero for $z \to -\infty$ reads $\rho_{ch} \propto \exp(z/\lambda)$. Near the surface, of course, there would be deviations from this behavior due to Friedel-like oscillations. Generalizing this idea to a spherical system and solving Eq. (11), we expect that the behavior of the charge density, far away from the surface, will be

$$\rho_{ch} \propto \frac{\sinh(r/\lambda)}{r/\lambda}\,. \tag{12}$$

Fitting λ to our solutions, we find that the fitted value for λ is indeed approximately the same for all large strangelets ($A \geq 15000$), namely $\lambda = 7.71 \ldots 7.76$ fm). This value is of the same order of magnitude as the photon Debye mass calculated from perturbative QCD, which reads, for the CFL phase, $m^2_{D,\gamma\gamma} = 1/\lambda^2 = 4\frac{21-8\ln 2}{54} e^2 N_f \mu^2/(6\pi^2)$ [20]. For typical values of the chemical potential this gives $\lambda \approx 10$ fm.

In principle, in color superconducting phases, the photon can mix with one of the gluons. In the CFL phase, in bulk matter, one linear combination of photon and gluon stays massless. This means that at large distances $d \gg 1/\Delta$, i.e., at distances much larger than the size of the Cooper pairs, the Debye screening for the "rotated" photon [21, 22] does not work, since the Cooper pairs are neutral with respect to the rotated charge $\tilde{Q}$. Within the simple model we use for the moment, there are no gluons,

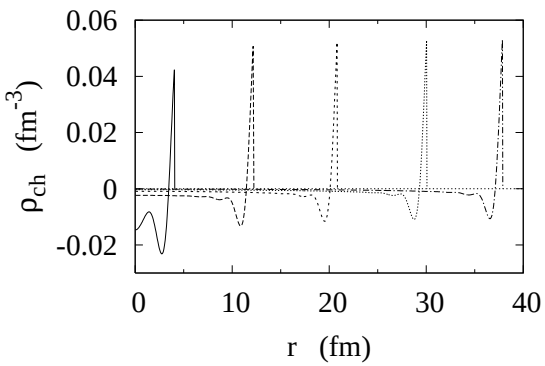

FIG. 8: Charge density profiles of the fully paired ($H\Lambda^2 = 2$) strangelets A =108, 3000, 15000, 45000, and 90000 (from left to right).

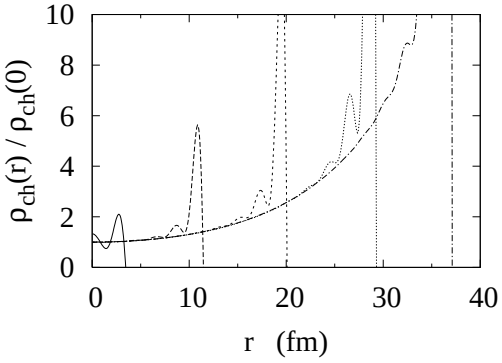

FIG. 9: Zoom into the part of Fig. 8 where the charge density behaves as given by Eq. (12). For a better visibility the charge densities have been divided by their respective values at $r = 0$.

such that the mixing cannot be studied. It could be taken into account, as mentioned at the end of Section II, by including the gluons in the same way as the photon, i.e., on the Hartree level. We expect that if we included the gluons in this way, we would find an even faster decrease of the charge if we go away from the surface, since in addition to the electromagnetic force we would have the color forces, which try to push the color charges to the surface, and in the CFL phase color neutrality goes hand in hand with electrical neutrality. Therefore, this is not in contradiction with the fact that the rotated photon is massless, but it is just a consequence of the fact that the combination of photon and gluon which is orthogonal to the rotated photon is massive (in fact, it is even heavier than the other gluons [22]). This means that in a large object, like a strange star, all the negative charge will be concentrated within a layer of a thickness of at most a few tens of fm below the surface. However, before drawing any firm conclusion, one should study this problem in more detail. This will be left for future work.

TABLE III: Fitted liquid-drop parameters for the CFL-type neutral strangelets ($Z = 0$). The surface tension σ corresponding to the fitted value of a_S is also given.

$B^{1/4}$ (MeV)	$H\Lambda^2$ (MeV)	a_S (MeV)	a_C (MeV)	σ (MeV/fm^2)
156.26	2	107	289	11.9
159.46	2.25	109	297	12.8
163.46	2.5	112	306	13.9

C. Liquid-drop type expansion

The advantage of the present approach is that finite size effects are correctly implemented. For large numbers of particles, this becomes, however, rather cumbersome and asymptotic expansions such as a liquid-drop type approach can be very useful. We will discuss here the determination of the parameters, such as the surface tension, of a liquid-drop type formula for the energy per baryon as a function of the baryon number A, including a surface and a curvature term,

$$\frac{E}{A} = \left(\frac{E}{A}\right)_{bulk} + \frac{a_S}{A^{1/3}} + \frac{a_C}{A^{2/3}}\,, \tag{13}$$

from our results.

As explained below Eq. (7), $(E/A)_{bulk}$ should be the energy per baryon of infinite matter with $\mu_e = 0$ rather than that of beta stable infinite matter. However, as in the preceding section, we restrict our discussion to the CFL-type solution, such that this distinction is irrelevant. Hence, for our chosen parameter sets, we have $(E/A)_{bulk} = 900$ MeV. Since for the neutral strangelets the Coulomb interaction has only a negligible effect on the total energies, it will be neglected in this section. The result of the fitted coefficients a_S and a_C for the different parameter sets are listed in Table III. As an example, in order to show the accuracy of the asymptotic expansion, we display in Fig. 10 some results for the energy per baryon together with the liquid-drop formula, Eq. (13). The dashed line corresponds to the liquid-drop formula without the curvature term ($a_C = 0$). From this figure it becomes clear that the liquid-drop formula with curvature term works extremely well, much better than in the case without pairing [23]. The reason is that shell effects are completely washed out because of the strong pairing (note that, contrary to the situation in ordinary nuclei, the pairing gap is larger than the spacing between neighboring shells). Another interesting observation is that the curvature term is very important, even for rather large mass numbers A.

The coefficient a_S is closely related to a very interesting quantity, namely the surface tension. As explained in Ref. [24], the surface tension is obtained as

$$\sigma = \frac{E_S}{4\pi R_0^2}\,, \tag{14}$$

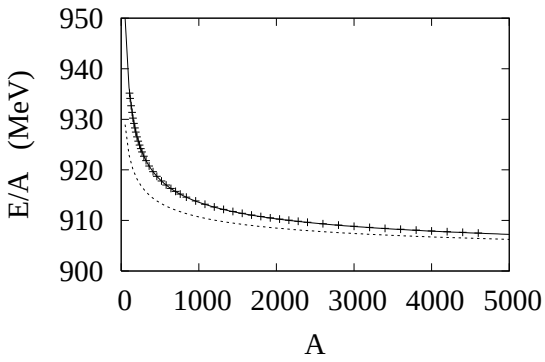

FIG. 10: Energy per baryon as a function of baryon number for $H\Lambda^2 = 2$ and $B^{1/4} = 156.26$ MeV. The exact results are indicated by the crosses, the fitted liquid-drop formula by the solid line. The dashed line corresponds to the liquid-drop formula without the curvature term.

where

$$E_S = E - A\left(\frac{E}{A}\right)_{bulk} \tag{15}$$

is the energy excess due to the surface and R_0 is an effective radius defined by

$$A = \rho_{B\,bulk}\frac{4\pi R_0^3}{3}\,, \tag{16}$$

which is actually very close to R for not too small strangelets. On the one hand, using the liquid-drop formula (13) for E in Eq. (14), one would obtain a surface tension which depends on A because of the curvature term. Therefore it is clear that one has to use Eq. (14) in the limit $A \to \infty$, where the curvature term vanishes, i.e.,

$$\sigma = \frac{a_S \rho_{B\,bulk}^{2/3}}{(36\pi)^{1/3}}\,. \tag{17}$$

The corresponding numbers are given in the last column of Table III. They are of the same order of magnitude as the estimate $\sigma \sim (70\ \mathrm{MeV})^3 = 8.8\ \mathrm{MeV/fm^2}$ for SQM without color superconductivity [25]. On the other hand, the fact that the curvature term is very strong implies that the knowledge of the surface tension alone might not be sufficient in order to determine, e.g., the possibility of mixed phases, the size of droplets, etc.

IV. SUMMARY

Within this paper we have investigated finite lumps of color superconducting strange quark matter. To that end we have solved the HFB equations. This allows to correctly include finite size effects for pairing, too.

Our main result is that, although the strange quark density is suppressed at the surface, the total charge of

the CFL type solution, as in bulk matter, is zero due to pairing. Including Coulomb effects, the positive surface charge on a length of approximately 1 fm is compensated by a negatively charged layer below the surface on a length scale of a few tens of fm. (This number will probably be strongly decreased if the gluons are included in a perturbative way similar to the photon). It remains to be investigated in which the way this changes the traditional picture of the surface of a strange star and the detectability of smaller strangelets in current experiments such as AMS-02 or LSSS [26].

We also compared our results for the energy per baryon of finite strangelets with a liquid-drop like formula. It turned out that, due to pairing, shell effects are strongly suppressed and the liquid-drop like formula is very precise. However, the curvature term is very large and its inclusion is crucial to reproduce the correct energies.

Acknowledgements

We thank Michael Buballa for useful discussions and for the critical reading of the manuscript.

APPENDIX A: SPINORS IN A SPHERICAL CAVITY

In this appendix we recall basic properties of free Dirac spinors in a spherical cavity (see, e.g., Ref. [27]). They can be written as

$$\psi_{fj\kappa mn}(\mathbf{r}) = \begin{pmatrix} g_{fj\kappa n}(r)\mathcal{Y}^m_{jl}(\Omega) \\ i\, f_{fj\kappa n}(r)\mathcal{Y}^m_{jl'}(\Omega) \end{pmatrix}, \tag{A1}$$

where $\mathcal{Y}$ are spinor spherical harmonics [28]. We have the following relations between the angular momentum quantum numbers

$$\begin{aligned} \kappa = j+\frac{1}{2} \quad &\rightarrow \quad l = j+\frac{1}{2}, \quad l' = j-\frac{1}{2} \\ \kappa = -(j+\frac{1}{2}) \quad &\rightarrow \quad l = j-\frac{1}{2}, \quad l' = j+\frac{1}{2}. \end{aligned} \tag{A2}$$

For the solutions of the free Dirac equation, the functions f and g are given as follows in terms of the spherical Bessel functions ($\xi_{fj\kappa n} = \sqrt{p^2_{fj\kappa n} + m_f^2}$)

$$\begin{aligned} g_{fj\kappa n}(r) =& C_{fj\kappa n}\, j_l(p_{fj\kappa n} r) \\ f_{fj\kappa n}(r) =& C_{fj\kappa n}\mathrm{sgn}(\kappa n)\sqrt{\frac{\xi_{fj\kappa n}-m_f}{\xi_{fj\kappa n}+m_f}}\, j_{l'}(p_{fj\kappa n} r), \end{aligned} \tag{A3}$$

where the $C_{fj\kappa n}$ are normalisation coefficients which can be determined from the normalization

$$\int_0^R dr r^2 \int d\Omega \psi^\dagger(\mathbf{r})\psi(\mathbf{r}) = 1. \tag{A4}$$

The momenta $p_{fj\kappa n}$ are obtained from the boundary condition. The boundary condition of the MIT bag model, Eq. (1), translates into the following equation

$$f_{fj\kappa n}(R) = -g_{fj\kappa n}(R), \tag{A5}$$

or, explicitly,

$$j_l(p_{fj\kappa n}R) = \mathrm{sgn}(\kappa n)\sqrt{\frac{\xi_{fj\kappa n}-m_f}{\xi_{fj\kappa n}+m_f}}\, j_{l'}(p_{fj\kappa n}R), \tag{A6}$$

where we number by $n > 0$ the positive-energy (particle) states and by $n < 0$ the negative-energy (antiparticle) states. In practice, we will keep only the states with positive eigenvalues and neglect the antiparticle contributions. The latter can approximately be absorbed into a redefintion of the coupling constant.

APPENDIX B: HFB EQUATIONS

In this appendix we will give some details about the HFB equations. Their derivation is analogous to the derivation of the Dirac-Hartree-Bogoliubov equations in finite nuclei, which is given in Ref. [18].

The HFB equations are derived from the Lagrangian by minimizing the energy in the mean field approximation, i.e., linearizing the interaction under the assumption of nonzero expectation values for the condensates $s_{AA'}(x)$, Eq. (2). Due to the inhomogeneities of a finite system, the Green's functions become nondiagonal in momentum. In the stationary case, it is convenient to work in $\mathbf{r}$ space for the spacial coordinates but to perform the Fourier transformation for the time variable. Then the Green's functions take the following general form in Nambu-Gorkov space:

$$\begin{aligned} S(\mathbf{x},\mathbf{y};\omega) &= \begin{pmatrix} G(\mathbf{x},\mathbf{y};\omega) & F(\mathbf{x},\mathbf{y};\omega) \\ \tilde{F}(\mathbf{x},\mathbf{y};\omega) & \tilde{G}(\mathbf{x},\mathbf{y};\omega) \end{pmatrix} \\ &= \sum_{\alpha(\epsilon_\alpha>0)} \begin{pmatrix} U_\alpha(\mathbf{x}) \\ V_\alpha(\mathbf{x}) \end{pmatrix} \frac{1}{\omega-\epsilon_\alpha+i\eta} (\bar{U}_\alpha(\mathbf{y}), \bar{V}_\alpha(\mathbf{y})) \\ &\quad + \sum_{\beta(\epsilon_\beta<0)} \begin{pmatrix} U_\beta(\mathbf{x}) \\ V_\beta(\mathbf{x}) \end{pmatrix} \frac{1}{\omega+\epsilon_\beta+i\eta} (\bar{U}_\beta(\mathbf{y}), \bar{V}_\beta(\mathbf{y})), \end{aligned}$$

where $G, \tilde{G}$ and $F, \tilde{F}$ are normal and anomal Green's functions, respectively. The spinors $U_{\alpha,\beta}$ and $V_{\alpha,\beta}$ correspond to the particle- and hole-like components, respectively.

All the necessary expectation values in mean-field approximation (like densities, particle numbers, total energy, etc.) can easily be expressed in terms of the U and V functions. To that end, it is sufficient to express the

expectation values in terms of the Green's functions, e.g.

$$\begin{aligned} s_{AA} &= -\langle\bar{\psi}_T(x)\tau_A\lambda_A\psi(x)\rangle \\ &= i\lim_{t\to 0^+}\mathrm{tr}F(0,\mathbf{r};t,\mathbf{r})\tau_A\lambda_A \\ &= -\sum_{\beta,\epsilon_\beta<0}\bar{V}_\beta(\mathbf{r})\tau_A\lambda_A U_\beta(\mathbf{r}) \end{aligned} \tag{B1}$$

By minimizing the total energy with respect to the U and V functions, one obtains the HFB equations, [see Eq. (5)]:

$$\mathcal{H}W_\alpha = \epsilon_\alpha W_\alpha\,, \tag{B2}$$

with $W_\alpha = (U_\alpha, V_\alpha)^T$.

For homogeneous infinite systems the matrix elements of $\mathcal{H}$ are diagonal in momentum space and solutions to the HFB equations are known for many cases. For finite systems, in general, these equations are solved numerically by diagonalizing the matrix $\mathcal{H}$ in some convieniently chosen basis. Here, we are working in the basis which diagonalizes h_{fc} (at least as long as the Coulomb interaction is neglected), see Appendix A, and the eigenvectors $U_\alpha(\mathbf{r})$ and $V_\alpha(\mathbf{r})$ are developped within this basis.

The matrix elements of the pairing fields $\Delta_A(r)$ (and of the Coulomb field $eA^0(r)$, if it is included) are computed in the usual way. For illustration, we give here the explicit expression for the matrix elements of $\Delta_2(r)$, which connects up (u) and down (d) quarks, in the basis described in Appendix A:

$$\begin{aligned} (\Delta_2)_{j\kappa nn'} &= \int d^3r\,\psi^\dagger_{uj\kappa mn}(\mathbf{r})\Delta_2(r)\psi_{dj\kappa mn'}(\mathbf{r}) \\ &= \int dr r^2\Delta_2(r)(g_{uj\kappa n}(r)g_{dj\kappa n'}(r) \\ &\qquad + f_{uj\kappa n}(r)f_{dj\kappa n'}(r))\,. \end{aligned} \tag{B3}$$

Note that, due to spherical symmetry, all matrices are diagonal in j and κ and proportional to the unit matrix with respect to m. The function $\Delta_2(r)$ is related to $s_{22}(r)$ via the gap equation, Eq. 6, i.e., it depends on the U and V functions. We therefore have to solve a self-consistency problem.

In spite of the spherical symmetry, the matrix to be diagonalized is still huge, limiting the number of particles which can be calculated with reasonable computational effort. It is therefore important to reduce the size of the actual matrix to be diagonalized. By means of an orthogonal transformation

$$\tilde{\mathcal{H}} = S\mathcal{H}S^T, \quad \tilde{W} = SW, \quad SS^T = 1 \tag{B4}$$

in color, flavor, and Nambu-Gorkov space, the matrix can actually be block-diagonalized (see, e.g., Ref. [29]) containing seven blocks. Six of them, $\tilde{\mathcal{H}}_{B,\ldots G}$, are 2×2 matrices in Nambu-Gorkov space, describing mutual pairing of two particles, such as for example red down quarks (dr) with green up quarks (ug):

$$\tilde{\mathcal{H}}_B = \begin{pmatrix} h_{ug} & \Delta_2 \\ \Delta_2 & -h_{dr} \end{pmatrix}, \tag{B5}$$

where h_{fc} is the single particle Hamiltonian for flavor f and color c. Since we have in addition the pairwise relations, $\tilde{\mathcal{H}}_{B,C,D} = -\tilde{\mathcal{H}}_{E,F,G}$, only three of these 2×2 matrices have to be diagonalized in practice. The seventh matrix, $\tilde{\mathcal{H}}_A$, is 6×6 in Nambu Gorkov space and describes pairing between red up, green down and blue strange quarks

$$\tilde{\mathcal{H}}_A = \begin{pmatrix} h_{ur} & 0 & 0 & 0 & \Delta_2 & \Delta_5 \\ 0 & h_{dg} & 0 & \Delta_2 & 0 & \Delta_7 \\ 0 & 0 & h_{sb} & \Delta_5 & \Delta_7 & 0 \\ 0 & \Delta_2 & \Delta_5 & -h_{ur} & 0 & 0 \\ \Delta_2 & 0 & \Delta_7 & 0 & -h_{dg} & 0 \\ \Delta_5 & \Delta_7 & 0 & 0 & 0 & -h_{sb} \end{pmatrix}. \tag{B6}$$

APPENDIX C: CUTOFF FOR THE GAP EQUATION

As mentioned in section II, the divergent gap equation is regularized with the help of a smooth cutoff function

$$f(p/\Lambda) = \frac{1}{1 + c_1\exp(c_2 a(p/\Lambda - 1))}\,, \tag{C1}$$

where $c_1 = \sqrt{2}-1$, $c_2 = 1/(4-2\sqrt{2})$, and $a = 22.58$ have been chosen such that $f^2(p/\Lambda)$ approximates the cutoff function $g(p/\Lambda)$ used in Ref. [30], but our function has the advantage to fall off more rapidly at very high momenta, which allows us to truncate the basis at a lower energy.

This function is used in the following symmetric way. First, when calculating $s_{AA}(r)$, and second, when calculating the matrix elements of $\Delta_A(r)$ in the basis of the spinors defined in Appendix A. It should be noted that the diagonalization of the HFB matrix does not directly provide us with the eigenfunctions $U_\alpha(\mathbf{r})$ and $V_\alpha(\mathbf{r})$, but with their respective expansion coefficients in the basis of the spinors defined in Appendix A. When calculating $s_{AA}(r)$ according to Eq. (6), the coefficients have to be multiplied with the corresponding basis functions, and in this step the factor $f(p_{fj\kappa n}/\Lambda)$ is attached to each basis function. Second, when calculating the matrix elements of the gap Δ_A, we again attach a factor $f(p_{fj\kappa n}/\Lambda)$ to each basis function.

[1] J.C. Collins and M.J. Perry, Phys. Rev. Lett. **34**, 1353 (1975); B. Barrois, Nucl. Phys. **B129**, 390 (1977); S.C. Frautschi, Asymptotic freedom and color superconduc-

tivity in dense quark matter, in: Proc. of the Workshop on Hadronic Matter at Extreme Energy Density, N. Cabibbo (ed.), Erice 1978; D. Bailin and A. Love, Phys. Rep. **107**, 325 (1984).
[2] M.G. Alford, K. Rajagopal, and F. Wilczek, Phys. Lett. B **422**, 247 (1998).
[3] R. Rapp, T. Schäfer, E.V. Shuryak, and M. Velkovsky, Phys. Rev. Lett. **81**, 53 (1998).
[4] K. Rajagopal and F. Wilczek, in: M. Shifman (Editor), *At the Frontier of Particle Physics, Handbook of QCD, Boris Ioffe Festschrift*, vol. 3, p. 2061 (World Scientific, Singapore 2001) [hep-ph/0011333]; M. Alford, Ann. Rev. Nucl. Part. Sci. **51**, 131 (2001); T. Schäfer, hep-ph/0304281; D.H. Rischke, Prog. Part. Nucl. Phys. **52**, 197 (2004); M. Buballa, Phys. Rep. **407**, 205 (2005); H.-C. Ren, hep-ph/0404074; M. Huang, Int. J. Mod. Phys. E **14**, 675 (2005); I. A. Shovkovy, Found. Phys. **35**, 1309 (2005).
[5] M.G. Alford, K. Rajagopal, and F. Wilczek, Nucl. Phys. **B 537**, 443 (1999).
[6] I.A. Shovkovy and L.C.R. Wijewardhana, Phys. Lett. B **470**, 189 (1999); T. Schäfer, Nucl. Phys. **B 575**, 269 (2000); N.J. Evans, J. Hormuzdiar, S.D.H. Hsu, and M. Schwetz, Nucl. Phys. **B 581**, 391 (2000).
[7] A.R. Bodmer, Phys. Rev. D **4**, 1601 (1971); E. Witten, Phys. Rev. D**30**, 272 (1984).
[8] C. Alcock, E. Farhi, and A. Olinto, Astrophys. J. **310**, 261 (1986); P. Haensel, J.L. Zdunik, and R. Schaeffer, Astron. Astrophys. **160**, 121 (1986).
[9] J. Madsen and J.M. Larsen, Phys. Rev. Lett. **90**, 121102 (2003); M. Rybczynski, Z. Wlodarczyk, and G. Wilk, Nucl. Phys. Proc. Suppl. **151**, 341 (2006).
[10] V.V. Usov, Phys. Rev. Lett. **80**, 230 (1998).
[11] D. Page and V.V. Usov, Phys. Rev. Lett.**89**, 131101 (2002).
[12] P. Jaikumar, S. Reddy and A.W. Steiner, Phys. Rev. Lett. **96**,041101 (2006).
[13] M.G. Alford, K. Rajagopal, S. Reddy, and A.W. Steiner, Phys. Rev. D **73**, 114016 (2006).
[14] K. Rajagopal and F. Wilczek, Phys. Rev. Lett. **86**, 3492 (2001).
[15] J. Madsen, Phys. Rev. Lett. **87**, 172003 (2001).
[16] V.V. Usov, Phys. Rev. D **70**, 067301 (2004).
[17] A. Chodos, R.L. Jaffe, K. Johnson, C.B. Thorn, and V.F. Weisskopf, Phys. Rev. D **9**, 3471 (1974).
[18] B.V. Carlson and D. Hirata, Phys. Rev. C **62**, 054310 (2000).
[19] W.V. Liu and F. Wilczek, Phys. Rev. Lett. **90**, 047002 (2003).
[20] A. Schmitt, Q. Wang and D.H. Rischke, Phys. Rev. D **69**, 094017 (2004).
[21] M.G. Alford, J. Berges, and K. Rajagopal, Nucl. Phys. **B 571**, 269 (2000)
[22] D.F. Litim and C. Manuel, Phys. Rev. D **64**, 094013 (2001).
[23] E.P. Gilson and R.L. Jaffe, Phys. Rev. Lett. **71**, 332 (1993).
[24] B.C. Parija, Phys. Rev. C **48**, 2483 (1993).
[25] E. Farhi and R.L. Jaffe, Phys. Rev. D **30**, 2379 (1984).
[26] J. Madsen, arXiv:astro-ph/0612784 (2006).
[27] R.K. Bhaduri, *Models of the Nucleon: From Quarks to Soliton* (Addison-Wesley, Redwood City 1988)
[28] D.A. Varshalovich, A.N. Moskalev, and V.K. Khersonskii, *Quantum Theory of Angular Momentum* (World Scientific, Singapore 1988).
[29] M.G. Alford, J. Berges, and K. Rajagopal, Nucl. Phys. B **558**, 219 (1999).
[30] S. Yasui and A. Hosaka, Phys. Rev. D **74**, 054036 (2006).